CHEMISTRY OF MATERIALS

Article

pubs.acs.org/cm

Highly Planarized Naphthalene Diimide–Bifuran Copolymers with Unexpected Charge Transport Performance

Rukiya Matsidik,[†,∥] Alessandro Luzio,[‡] Özge Askin,[‡] Daniele Fazzi,[§] Alessandro Sepe,[◇] Ullrich Steiner,[◇] Hartmut Komber,[⊥] Mario Caironi,*[,‡] and Michael Sommer*[,†,∥,#,○]

[†]Universität Freiburg, Institut für Makromolekulare Chemie, Stefan-Meier-Str. 31, 79104 Freiburg, Germany

[∥]Freiburger Materialforschungszentrum, Stefan-Meier-Str. 21, 79104 Freiburg, Germany

[‡]Center for Nano Science and Technology @PoliMi, Istituto Italiano di Tecnologia, Via Pascoli 70/3, 20133 Milano, Italy

[§]Max-Planck-Institut für Kohlenforschung (MPI-KOFO), Kaiser-Wilhelm-Platz 1, D-45470 Mülheim an der Ruhr, Germany

[◇]Adolphe Merkle Institute, University of Fribourg, Chemin des Verdiers 4, CH-1700 Fribourg, Switzerland

[⊥]Leibniz Institut für Polymerforschung Dresden e.V., Hohe Straße 6, 01069 Dresden, Germany

[#]FIT Freiburger Zentrum für interaktive Werkstoffe und bioinspirierte Technologien, Georges-Köhler-Allee 105, 79110 Freiburg, Germany

Supporting Information

ABSTRACT: The synthesis, characterization, and charge transport performance of novel copolymers PNDIFu2 made from alternating naphthalene diimide (NDI) and bifuran (Fu2) units are reported. Usage of potentially biomass-derived Fu2 as alternating repeat unit enables flattened polymer backbones due to reduced steric interactions between the imide oxygens and Fu2 units, as seen by density functional theory (DFT) calculations and UV–vis spectroscopy. Aggregation of PNDIFu2 in solution is enhanced if compared to the analogous NDI–bithiophene (T2) copolymers PNDIT2, occurring in all solvents and temperatures probed. PNDIFu2 features a smaller $\pi-\pi$ stacking distance of 0.35 nm compared to 0.39 nm seen for PNDIT2. Alignment of aggregates in films is achieved by using off-center spin coating, whereby PNDIFu2 exhibits a stronger dichroic ratio and transport anisotropy in field-effect transistors (FET) compared to PNDIT2, with an overall good electron mobility of 0.21 $cm^2/(V\ s)$. Despite an enhanced backbone planarity, the smaller $\pi-\pi$ stacking and the enhanced charge transport anisotropy, the electron mobility of PNDIFu2 is about three times lower compared to PNDIT2. Density functional theory calculations suggest that charge transport in PNDIFu2 is limited by enhanced polaron localization compared to PNDIT2.

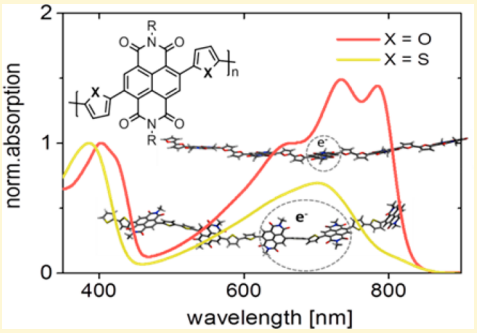

1. INTRODUCTION

In the exploration of polymer semiconductors for organic electronics, good hole conducting conjugated polymers have been extensively studied making high-performance p-type devices available in manifold variations. Good electron conducting or electron accepting conjugated polymers are increasingly investigated but still limited in terms of structural diversity.[1−3] Electron deficient structures, such as diketopyrrolopyrrole (DPP),[4] perylene diimide (PDI),[5] naphthalene diimide (NDI),[6] pyromellitic acid diimide,[7,8] benzodifurandione-based oligo(*p*-phenylenevinylene),[9,10] and their derivatives are most often incorporated into polymer backbones to achieve suitable n-channel properties in electronic devices.[1,3,11] DPP-based conjugated polymers mostly exhibit ambipolar properties in common field-effect transistor (FET) devices, with usually higher p-type than n-type performance.[11] The synthesis of PDI-based copolymers is challenging due to difficulties in separating isomers.[12] NDI derivatives can be relatively easily incorporated into polymer backbones using various synthetic approaches[6,13,14] and have thus become prime building blocks in materials for n-channel devices. In 2009, Yan et al. reported high electron-mobilities for NDI bithiophene (T2) copolymers, known as PNDI2OD-T2 and herein referred to as PNDIT2, which triggered tremendous interest in NDI-based polymers for use in n-type devices.[15] Since then, PNDIT2 has been the subject of many fundamental investigations regarding electronic structure, morphology and device performance.[16−22] Meanwhile, many derivatives of PNDIT2 have been synthesized.[6,23,24] Interestingly, only a few isolated examples outperformed PNDIT2,[23,25,26] while other comonomer structures did not lead to enhanced performance. Indeed, thiophene (T) is a simple, cost-efficient, well-explored, and extremely versatile building block used in conjugated polymers. Compared to the overwhelming presence

Received: December 15, 2016
Revised: June 9, 2017
Published: June 13, 2017

DOI: 10.1021/acs.chemmater.6b05313
Chem. Mater. 2017, 29, 5473−5483

of thiophene in conjugated materials, its oxygen analogue furan (Fu) has received much less attention despite its advantageous properties.[27,28] For example, Fu is available from biomass[29] and gives materials with improved solubility.[23,30] In cases in which sterical hindrance between thiophene and adjacent aromatic units lowers conjugation by increased torsion, the smaller size of furan can lead to enhanced planarization, which is thought to allow smaller $\pi-\pi$ stacking distances and eventually improved charge transport performance.[23,31] A drawback of furan-based copolymers is their reduced thermal stability that arises from the decreased aromatic character of furan, which might have contributed to the limited deployment of furan-based (co)-polymers in material science.[29] We have recently reported that the incorporation of FuNDIFu, which is a π-extended monomer of NDI unit flanked with furan, into conjugated polymers with tetrafluorobenzene F_4 leading to PNDIFu$_2$F$_4$ allowed for a reduced $\pi-\pi$ stacking distance compared to the thiophene analogue PNDIT$_2$F$_4$.[23] However, contrary to the general assumption that smaller $\pi-\pi$ stacking distances are beneficial for enhanced electron transport, the thiophene analogue PNDIT$_2$F$_4$ showed higher electron mobilities as a result of beneficial long-range ordering.[23] Further investigations have compared furan-based structures with their thiophene analogues with mixed outcomes. While some furan-derived structures showed enhanced performance,[32,33] others showed adverse results with furan-based small molecules and DPP copolymers exhibiting reduced mobilities.[34−36] Thus, the impact of replacing thiophene with furan can vary greatly depending on the system and structure under scrutiny. In order to investigate structure−function relationships resulting upon replacing thiophene by furan in main chain NDI copolymers, we synthesized the bifuran analogue of PNDIT2 with two different side chains, namely, 2-hexyloctyl (PNDIFu2-C16) and 2-octyldodecyl (PNDIFu2-C20), using a nickel-catalyzed polymerization of radical anions as shown in Scheme 1. Interestingly, while the higher chalcogen analogue of PNDIT2 having a biselenophene comonomer is known, PNDIFu2 has not yet been reported.[37]

Scheme 1. Reaction Scheme for the Synthesis of PNDIFu2 and PNDIT2[a]

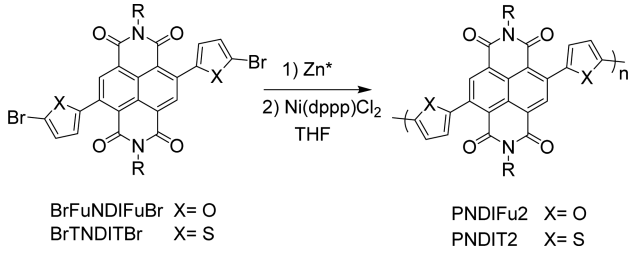

BrFuNDIFuBr X= O
BrTNDITBr X= S

PNDIFu2 X= O
PNDIT2 X= S

[a]R = 2-hexyldecyl or 2-octyldodecyl.

For comparison, the thiophene analogues PNDIT2-C16 and PNDIT2-C20 with the same side chains were prepared as well. In a comparative study, we explain how the replacement of sulfur in PNDIT2 by oxygen leading to PNDIFu2 changes the optical, structural, and electronic properties of the material along with the effect of a side chain length variation. We fabricate FETs from directionally deposited films to investigate how the changes in properties are reflected by their electron transport performance.

2. RESULTS AND DISCUSSION

Previously, we observed that the reduced steric hindrance between furan and NDI, as caused by the smaller size of furan, is responsible for a lowered torsion angle of 19° in FuNDIFu compared to 42° in TNDIT.[31] We envisioned the lower torsional angle in FuNDIFu to be a key parameter for enhancing backbone planarity, aggregation, thermal behavior, solid state structure, and eventually electronic performance. Therefore, a series of NDI copolymers with alternating bifuran and bithiophene units and two different side chains, referred to as PNDIFu2-C16, PNDIT2-C16, PNDIFu2-C20, and PNDIT2-C20, were made with comparably similar molecular weight of $M_{n,SEC} \approx$ 16, 17, 18, and 17 kDa, respectively. Usage of the shorter 2-hexyldecyl side chain was motivated by generally enhanced solubility of furan-based materials,[30] which however will be shown not to be the case.

2.1. Polymer Synthesis. The synthesis of the π-extended monomers, FuNDIFu and TNDIT, was straightforward via direct arylation using an excess of furan or thiophene.[31] Bromination of FuNDIFu with NBS was efficient at room temperature, while the analogue reaction of TNDIT required elevated temperature of 60 °C. Purification of both monomer precursors was achieved by recrystallization from ethanol, giving high isolated yields of 85% (C16) and 92% (C20) for BrFuNDIFuBr, and 90% (C16 and C20) for BrTNDITBr (see Supporting Information). Polymerization was carried out using activation with Rieke zinc to generate radical anions followed by the subsequent addition of NidpppCl$_2$ (Scheme 1).[38] However, contrary to the previously reported mechanism including partial chain-growth character, low catalyst loadings led to low molecular weights in the case of PNDIFu2. A similar issue was also reported for KCTP of poly(3-hexylfuran) due to strong aggregation.[39] Increasing the catalyst loading to 10 mol %, molecular weights of $M_n \approx$ 17 kDa were readily achieved after 1 h with high conversion and yield (~90%). However, early precipitation of PNDIFu2 occurred as well as a result of significant aggregation. Monitoring the reaction kinetics by taking aliquots during polymerization and analyzing them by size exclusion chromatography (SEC) showed that the starting monomer was completely consumed after 30 min (Figure S1). Most likely, subsequent coupling of prepolymerized Br(FuNDI-Fu)nBr segments may have led to high molecular weight and precipitation, whereby the yield of soluble product can be maximized by reducing the reaction time, thus limiting precipitation.[40] To enable high yields and overcome issues with precipitation, target molecular weights for this comparative study were set to $M_{n,SEC} \approx$ 17 kg/mol. Thus, a set of three samples, referred to as PNDIFu2-C16, PNDIFu2-C20, PNDIT2-C16, with $M_{n,SEC} \approx$ 16, 17, 18, kDa, respectively, and dispersities around 2.4 were prepared using NidpppCl$_2$.

A fourth sample PNDIT2-C20, albeit synthesized by direct arylation polycondensation,[14] exhibits the same structural integrity as PNDIT2-C16, based on high-temperature ^{1}H NMR spectroscopy and SEC, and can thus be used for comparison (Table 1).

2.2. Intramolecular Structure: Insights into Neutral and Charged States from DFT Calculations. Gas-phase DFT calculations were first carried out to get insight into the geometric and electronic structure of PNDIFu2 to highlight the differences that arise from the replacement of T with Fu. Both the repeat units (i.e., monomer, n = 1) and the oligomers (i.e., five repeat units, n = 5) of PNDIFu2 and PNDIT2 were

DOI: 10.1021/acs.chemmater.6b05313
Chem. Mater. 2017, 29, 5473−5483

Table 1. Summary of Physical, Thermal, Optical, Electrical, and Structural Properties of PNDIX2-R (X = Fu, T; R = C16, C20)

polymer	$M_{n,SEC}$ /Đ [kDa][a]/[−]	T_m [°C]	T_c [°C]	T_{onset} [°C]	E_{LUMO}/E_{HOMO} [eV][b]	$E_{g,elec}$ [eV][b]	$E_{g,opt}$ [eV][c]	$E_{g,opt}$ [eV][d]	$E_{g,opt}$ [eV][e]	(100) spacing [nm][f]	CL [nm][g]	$\pi-\pi$ distance [Å][f]
PNDIFu2-C16	17/2.24	n.d.	n.d.	390	−3.77/−5.59	1.82	1.66	1.48	1.46	2.25	14.14	3.68
PNDIT2-C16	18/3.28	341	318	445	−3.82/−5.67	1.97	1.75	1.46	1.46	2.12	10.28	3.94
PNDIFu2-C20	16/2.38	n.d.	n.d.	390	−3.76/−5.79	1.91	1.68	1.49	1.47	2.90	14.50	3.55
PNDIT2-C20	17/2.35	298	288	445	−3.78/−5.81	2.03	1.75	1.61	1.47	2.52	8.08	3.86

[a]From size exclusion chromatography (SEC) in chloroform at room temperature. [b]From CV of thin films, average value from three measurements. [c]From the onset of absorption: in CN at room temperature for PNDIT2 and at 170 °C for PNDIFu2. [d]From the onset of absorption in toluene at room temperature. [e]From the onset of absorption in film. [f]GIWAXS data from PNDIFu2 and PNDITh2 films annealed at 250 and 100 °C, respectively. [g]Coherence length (CL) for the 100 reflection (face-on orientation).

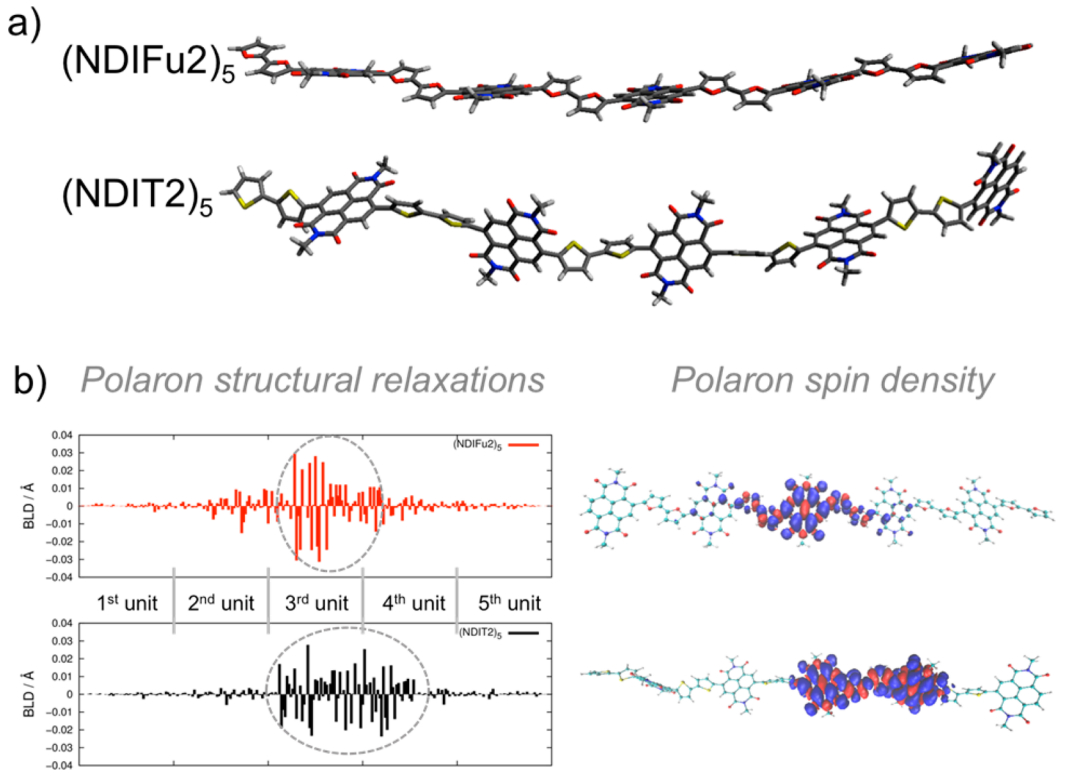

Figure 1. (a) DFT (ωB97X-D/6-311++G*) optimized ground state structures for model pentamers $(NDIFu2)_5$ and $(NDIT2)_5$. (b, left) Bond length differences (BLD) between each bond in the charged (elec) with respect to the neutral state, for $(NDIFu2)_5$ and $(NDIT2)_5$. For the sake of clarity, the extension and number of each repeat unit of the two polymers are reported. The polaron structural distortions are highlighted with circles (dashed gray line) to guide the eye. (b, right) Computed polaron spin density for $(NDIFu2)_5$ and $(NDIT2)_5$.

considered. Relaxed DFT potential energy profile calculations (ωB97X-D/6-311++G*), along the dihedral coordinate (τ) connecting the NDI unit with Fu or T rings were computed for the monomers, revealing an asymmetric double well potential[17,22] with stable conformations around τ = 28° (or 152°) for NDI-Fu and τ = 42° (or 138°) for NDI-T. At the monomer level, FuNDIFu features a more planar structure than TNDIT. To model the structure of the polymers' backbone, we built up conformationally regular oligomer chains $(NDIFu2)_5$ and $(NDIT2)_5$ with five repeat units. The ground state (neutral) DFT equilibrium molecular structures are reported in Figure 1a. $(NDIFu2)_5$ features a planar and flat structure. On the contrary, $(NDIT2)_5$ shows tilted conformations that lead to out-of-plane distortions between the NDI and T2. We believe the more planar structure of $(NDIFu2)_5$ and the distorted one of $(NDIT2)_5$ are intrinsic structural properties of the polymers, as calculations were intentionally carried out without the presence of any other interacting molecules or chains. In general care needs to be taken when comparing gas-phase calculations with experimental data. However, previous studies on PNDIT2[41,42] have already shown that this polymer can give coiled configurations in solution. The planar structure of PNDIFu2 would allow for a strong tendency to aggregate via stabilized $\pi-\pi$ and van der Waals interactions. This feature is actually observed and will be discussed in the following paragraphs. A more planar polymer backbone leads to a red-shifted absorption band in the electronic transitions and UV−vis spectra, as computed and observed for PNDIFu2 with respect to PNDIT2 (see Figure 3 and Supporting Information). From the analysis of the molecular orbitals involved in the S0−S1 transition, we can deduce that the substitution of bithiophene with bifuran does not alter the character of the

DOI: 10.1021/acs.chemmater.6b05313
Chem. Mater. 2017, 29, 5473−5483

excited state, prevalently involving the HOMO → LUMO and the HOMO−1 → LUMO+1 contributions for both PNDIFu2 and PNDIT2. Frontier occupied molecular orbitals (e.g., HOMO−1, HOMO) are mainly localized on the donor units (i.e., bifuran and bithiophene), whereas the unoccupied (e.g., LUMO, LUMO+1) are on the acceptor NDI unit (see the isosurfaces reported in the Supporting Information). Due to the change in the electron density during the S0−S1 excitation, as suggested by the analysis of the molecular orbitals, the first absorption band can be assigned to a charge-transfer excitation for both polymers, with the transition dipole moment oscillating along the polymer axis.[43]

To get insights in the charged electronic state, we computed the molecular structures for the charged species (here referred to as polarons) of $(NDIFu2)_5$ and $(NDIT2)_5$. In the charged states (i.e., anion) structural polaron relaxations occur,[16] as reported in Figure 1b for $(NDIFu2)_5$ and $(NDIT2)_5$. The structural relaxations are computed as bond length differences (BLD) between the structures in the charged and in the neutral state. In $(NDIFu2)_5$, the polaron is prevalently localized over a single polymer unit, while in $(NDIT2)_5$ it is more delocalized, covering almost two polymer repeat units. A different polaron extension is also reflected by the polaron spin density, as reported in Figure 1b for both polymers. As a consequence of a different polaron extension, the computed electron intramolecular reorganization energy (λ^{elec}) is higher for $(NDIFu2)_5$ than for $(NDIT2)_5$, namely, 0.52 and 0.40 eV, respectively. This is due to the fact that the overall structural reorganizations (i.e., bond length and bond angle variations) are occurring over the single unit for the furan-based oligomers, while over a more extended segment length for PNDIT2. Although this is not the aim of the current study and more detailed investigations will be pursued in this direction, a different polaron extension might lead to a different transport regime, according to the small polaron and large polaron descriptions.[44,45]

In a first and qualitative approximation (i.e., homogeneous electron transfer reaction and similar electronic coupling integrals), the calculation of the intramolecular reorganization energy can suggest a lower electron mobility for PNDIFu2 compared to PNDIT2, despite the more planar ground state conformation of the former. Regardless of the kind of charge transport regime (e.g., Marcus, variable-range-hopping, small/large polaron, coherent/incoherent transport),[46] the calculation of the intramolecular reorganization energy suggests a slower intrachain electron transfer process for PNDIFu2 compared to PNDIT2. This conclusion might be correlated with the measured electron mobility, which is lower for PNDIFu2 than PNDIT2 (see section 2.6); however, more appropriate multiscale computational investigations should be carried out before addressing the correct charge transport regime.[47,48]

2.3. Aggregation in Solution and Optical Properties.

To further investigate aggregation behavior in detail, we measured temperature-dependent NMR spectroscopy of PNDIT2 and PNDIFu2 at different temperatures. PNDIT2 is known to give very narrow signals in tetrachloroethane at 120 °C, suggesting molecularly dissolved chains.[14]

Figure 2 shows ^{1}H NMR spectra of PNDIFu2-C16 and PNDIT2-C16 at different temperatures but at the same concentration of 10 mg/mL. Marked qualitative differences are spotted between PNDIFu2-C16 and PNDIT2-C16. At 30 °C both polymers showed broadened signals indicating aggregation.[42] While for PNDIT2-C16 the additional signals

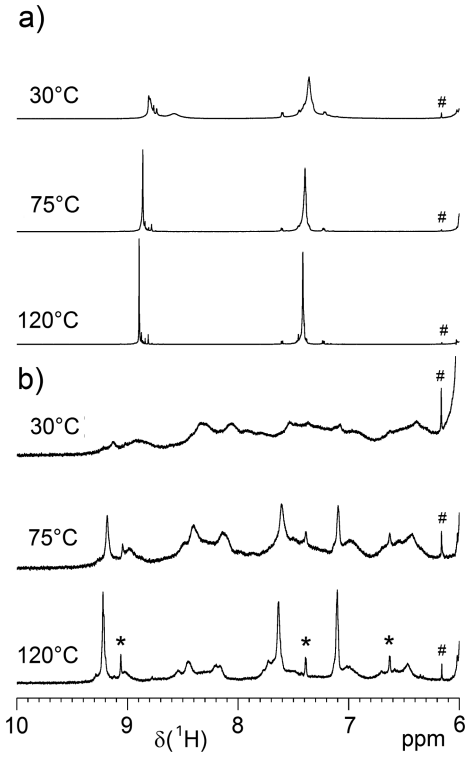

Figure 2. Temperature-dependent ^{1}H NMR spectra (aromatic region) of (a) PNDIT2-C16 and (b) PNDIFu2-C16. The polymer concentrations are 10 mg/mL in $C_2D_2Cl_4$. *Signals of the −NDI-Fu-Br end group; $^{\#13}$C satellite signal of the solvent.

arising from aggregation vanished already at T > 75 °C and narrow signals were observed at 120 °C suggesting molecularly dissolved chains,[14] this effect is much less pronounced for PNDIFu2-C16. Here, a strong aggregation was observed in tetrachloroethane even at 120 °C. This hampers signal assignment; however, the three narrow signals at 9.23, 7.64, and 7.11 ppm are characteristic of the PNDIFu2 backbone. Additionally, signals of 2-bromofuran end groups appeared (Figure 2b). Cooling solutions of PNDIFu2-C16 from 120 °C reproduced the ^{1}H NMR spectra, suggesting that the various signals arise from aggregation and not from temperature-induced decomposition of PNDIFu2.

Temperature-dependent UV−vis spectroscopy is an effective method to investigate aggregation in solution. Aggregation behavior of PNDIT2 was previously investigated by Steyrleuthner et al. showing strong aggregation in toluene and molecularly dissolved chains in 1-chloronaphthalene (CN).[42] Figure 3 shows solution absorption spectra of PNDIFu2 and PNDIT2 in CN and in toluene at room temperature and in film, which display marked differences between PNDIFu2 and PNDIT2. In CN (Figure 3a), the low energy absorption charge transfer (CT) band of PNDIFu2 is red-shifted by 66 nm compared to PNDIT2, and the intensity ratio between the CT and the high-energy band is much higher for PNDIFu2 than PNDIT2. Additionally, PNDIFu2-C20 displays a shoulder in the lower energy band, while in PNDIFu2-C16 it turns into a marked absorption band, pointing to strong aggregation even in CN, a solvent in which PNDIT2-C20 does not aggregate.[42] PNDIT2-C16 has an absorption spectrum very similar to PNDIT2-C20 in CN, with a slightly higher intensity ratio between the CT and the high-energy band than PNDIT2-C20. In the preaggregating solvent toluene (Figure 3b, solid line),

DOI: 10.1021/acs.chemmater.6b05313
Chem. Mater. 2017, 29, 5473−5483

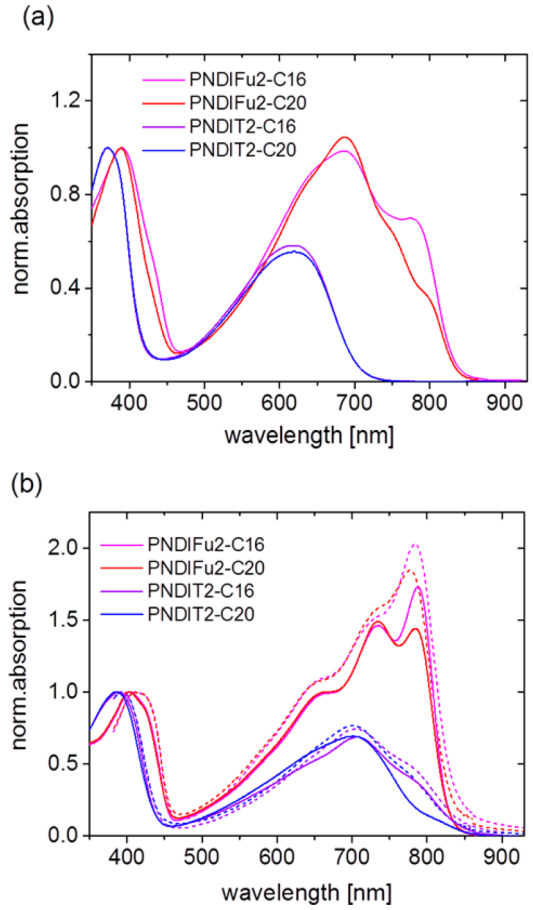

Figure 3. UV−vis absorption spectra of polymers in 1-chloronaphthalene (a), in toluene (b, solid line) at room temperature, and in film state (b, dashed line).

however, the absorption bands of PNDIT2 are clearly red-shifted. Moreover, in toluene, the difference between the two different side chains is more obvious for PNDIT2 than for PNDIFu2. Both PNDIFu2 polymers give same onset in toluene as in CN, while the shape of absorption is completely different. Further solvents are also investigated, which show similar behavior as in toluene (Figure S2). In thin films, all four polymers exhibit almost the same absorption onset regardless of heteroatoms and side chains, while the absorption intensity and the shape of the absorption band vary with respect to the type of heteroatom. PNDIT2-C20 is known to have similar absorption features in solid state and in preaggregating solvents.[42] This is found to be also the case for PNDIFu2. In order to further investigate aggregation behavior of the polymers, we conducted temperature-dependent UV−vis measurements in CN and in 1,2,4-trichlorobenzene (TCB). The spectra of PNDIFu2-C16 and PNDIT2-C16 are shown in Figure 4 as an example. In CN, increasing the temperature induces minor changes in the absorption features of PNDIT2-C16, while PNDIFu2-C16 showed a continuous decrease of the long-wavelength peak which completely disappeared at 170 °C. In TCB, PNDIT2-C16 shows distinct long-wavelength shoulders that disappeared at 90 °C, while PNDIFu2-C16 again required a much higher temperature of 190 °C to reach a molecularly dissolved state, confirming that aggregation of PNDIFu2 is much stronger than that of PNDIT2. The extracted optical energy gaps $E_{g,opt}$ from molecularly dissolved, preaggregated solutions and from the film state mirror the absorption changes between PNDIFu2 and PNDIT2 in different conditions, as collected in Table 1. Molecularly dissolved PNDIFu2 has a smaller $E_{g,opt}$ than PNDIT2, indicating enhanced NDI-Fu intramolecular coupling compared to NDI-T. However, the difference between PNDIFu2 and PNDIT2 in terms of optical absorption onset obtained from preaggregating solutions and in film is reduced, leading to similar energy values. The electrical band gaps ($E_{g,elec}$), calculated from cyclic voltammetry, were smaller for PNDIFu2 than PNDIT2, while the shape of oxidation and reduction peaks was similar in all polymers (Figure S3).The Fu2 or T2 comonomer mostly affects the HOMO energy level, with PNDIFu2 having a higher HOMO energy level than PNDIT2 (Table 1).

2.4. Thermal Properties. To study thermal stability, we measured thermal gravimetric analysis (TGA) and differential scanning calorimetry (DSC) (Table 1 and Figure S4). From TGA, regardless of the side chain length, PNDIT2 polymers showed a higher thermal stability than PNDIFu2, giving decomposition temperatures at around 445 and 390 °C, respectively. Thus, the degradation temperature of PNDIFu2 is lower but still appreciably high. We found PNDIFu2 to be stable in air when stored as solid/film with no degradation being observed within two years. However, in solution, PNDIFu2 is sensitive to light and starts to degrade within 2 weeks (if stored under day light). Replacing T2 by Fu2 again showed marked differences in the melting (T_m) and crystallization temperatures (T_c) (Figure S4). PNDIT2 owns clear T_m and T_c with distinct differences between two different side chains. Usage of the shorter side chains increases T_m of PNDIT2-C16 significantly from 298 °C commonly found for PNDIT2-C20[14] to 341 °C. PNDIFu2 polymers did not show T_m and T_c within the temperature range tested, with temperatures higher than 380 °C not being accessible because of potential decomposition. It is likely that the increased aggregation in PNDIFu2 leads to much higher T_m values that cannot be probed by conventional DSC experiments.

2.5. Thin Film Morphology. To obtain more insights into the structural properties, we investigated all samples by grazing incidence wide-angle X-ray scattering (GIWAXS), giving access to information about molecular packing. Structural changes upon thermal annealing were also examined. Figure 5 represents GIWAXS scattering pattern of as-spun and annealed films with different annealing conditions consistent with later FET preparation temperatures are found in Figures S5 and S6. The vertical integration shows the *a*-axis (100) reflections being edge-on and $\pi-\pi$ stacking directions (010) being face-on oriented.

Horizontal integration represents the evolution of the *a*-axis face-on and $\pi-\pi$ stacking edge-on oriented. As it can be seen from Figure 5, as-spun films (solid lines) of all four polymers showed short-range order with mixed orientations including edge-on, face-on, and random orientations with respect to the substrate, with PNDIT2 films showing more oriented crystallites than PNDIFu2 ones. Thermal treatment was not effective for PNDIFu2 films, while PNDIT2 showed the known transition from face-on to edge-on with increasing temperature,[49] with both C16 and C20 side chains giving comparable effects. Up to five orders of (h00) reflections are observed in the vertical direction when PNDIT2 films are subjected to 300 °C annealing, indicating significant order of edge-on oriented conjugated segments along the *a*-axis. However, the effect of furan and side chain length is more predominantly reflected by

DOI: 10.1021/acs.chemmater.6b05313
Chem. Mater. 2017, 29, 5473−5483

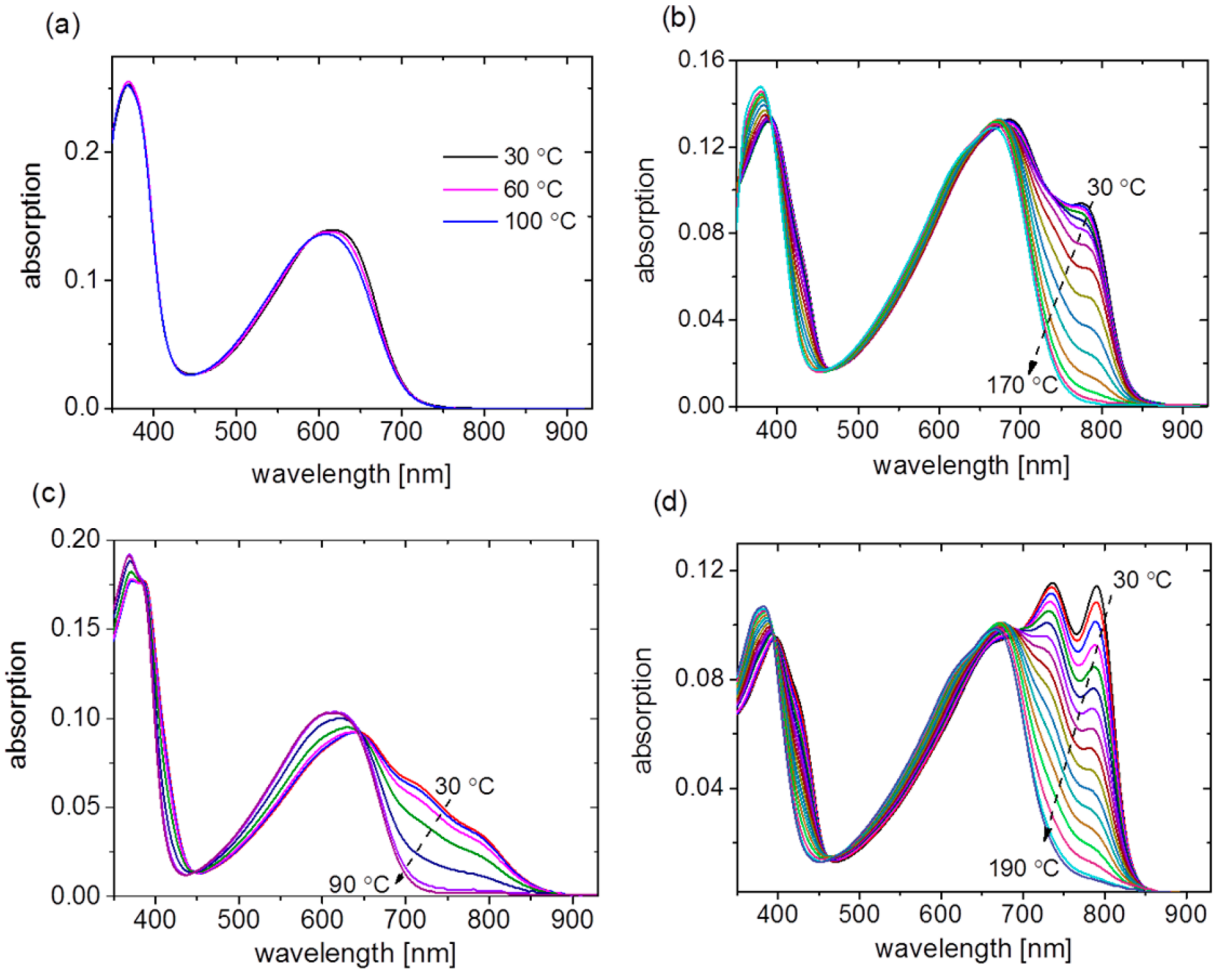

Figure 4. Temperature-dependent UV−vis absorption of PNDIT2-C16 (a,c) and PNDIF2-C16 (b,d) in 1-chloronaphthalene (a,b) and in trichlorobenzene (c,d).

the (100) spacing and $\pi-\pi$ stacking distance. For both PNDIFu2 and PNDIT2, in agreement with the side chain length, a larger (100) spacing was observed for the larger side chain 2-octyldodecyl (C20) compared to C16 chain. Additionally, this side chain effect on the (100) spacing is more predominant for PNDIFu2 than PNDIT2 as listed in Table 1. Clear $\pi-\pi$ stacking peaks are also observed for all polymers, with a significantly smaller $\pi-\pi$ staking distance for PNDIFu2 (0.35 nm for C16, and 0.37 nm for C20), compared to PNDIT2 (0.39 nm for C16 and C20). The former is in agreement with the enhanced coplanar structure of PNDIFu2 that if persisting in the solid state can be caused by the smaller torsional angle between NDI and Fu2.

2.6. Charge Transport in Field-Effect Transistors. The charge transport properties of the copolymers were investigated using top-gate bottom-contact (TGBC) field effect transistors (FETs) (Figure 6a). In light of recent observations of charge transport anisotropy in polymeric films simply controlled using directional flow during film deposition (negligibly affecting crystallographic parameters[50]), the thin films were deposited using off-center spin coating,[14,51] as sketched in Figure 6b. Transport anisotropy can then be evaluated comparing transport properties parallel (Figure 6c, channel configuration A) and perpendicular (Figure 6c, channel configuration B) to the flow of the solution. In order to confidently establish the effect of the two donor moieties on performance, preliminary investigations were carried out aimed at optimizing solution formulation and annealing temperatures independently (Figures S7 and S8). It is worth noting that given the intrinsic anisotropic nature of the thin films processed from preaggregated solutions,[19] probing transport on uniaxially aligned films is more representative than in films with random distributed orientational domains, as obtained by a common, centered spin-coating deposition. In agreement with previous reports on PNDIT2-C20, negligible dependence of FET behavior on annealing temperature was found.[49,52,53] Differently, FET transport in PNDIFu2 is maximized upon annealing at 250 °C for 30 min, while a drop of field effect mobility is observed by using annealing temperatures $T \geq 300$ °C, which might be related to thermal degradation even though thermal decomposition occurred at 390 °C according to TGA measurements. Concerning solution formulation, both PNDIT2-C20[19] and PNDIFu2-C20 gave best FET results using toluene (in terms of mobility and transport anisotropy). Differently, the best performance for PNDIT2-C16 and PNDIFu2-C16 was obtained using chlorobenzene (CB) and 1,2-dichlorobenzene (o-DCB) solutions, respectively (Figure S8). Typical electron accumulation *n*-type channel behavior is observed in all FETs of this work, each polymer displaying superior source to drain currents (I_{DS}) in A channel configuration than in B, as expected in case of flow-directed orientational alignment.[53] In Figure 6 the transfer curves (d)

DOI: 10.1021/acs.chemmater.6b05313
Chem. Mater. 2017, 29, 5473−5483

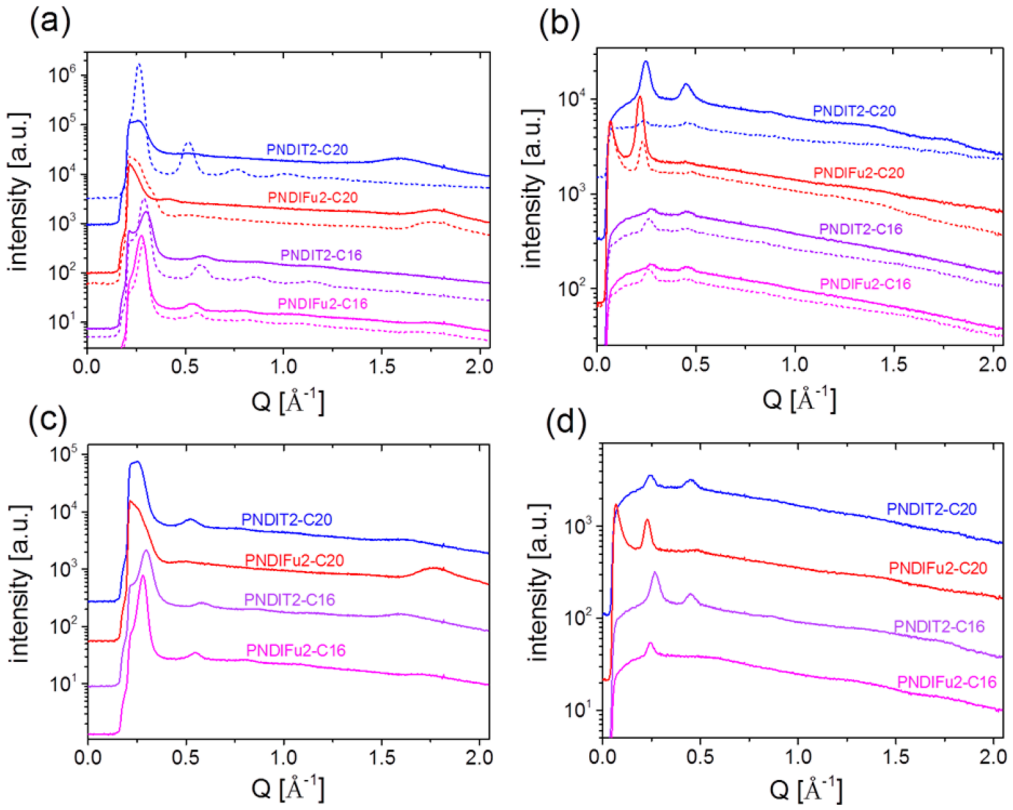

Figure 5. One-dimensional GIWAXS scattering vertical (a,c) and horizontal (b,d) integration profiles of polymer films: (a,b) as-spun (solid line) and annealed at 300 °C (dashed line) films; (c,d) films annealed at 100 °C (PNDIT2) and at 250 °C (PNDIFu2) corresponding to FET preparation.

and the corresponding extracted mobility values (e), obtained after a thorough process optimization, are reported and compared. It can be observed that for equal side chains PNDIFu2 displays a stronger anisotropy than PNDIT2 (molecular alignment investigation carried out through polarized UV−vis measurements is also reported in Figure S9).

This is in agreement with PNDIFu2 showing superior aggregation in solution, which seeds the long-range directional alignment in flow aligned films.[19,51] $I_{DS,A}/I_{DS,B}$ values (V_{GS} = 60 V) of 8.7 and 18.3 were extracted for PNDIFu2-C16 and PNDIFu2-C20, respectively, and 2.69 and 4.9 for PNDIT2-C16 and PNDIT2-C20, respectively. It is noteworthy that C20 side chains result in stronger transport anisotropy both for PNDIFu2 and PNDIT2, potentially due to a stronger nematic liquid-crystalline character of the lyotropic solutions induced using bulkier side chains.[54] In terms of absolute electron mobilities, the best PNDIT2 FETs displayed an approximately three times higher mobility than the best PNDIFu2 devices: we extracted similar $\mu_{sat,max}$ of 0.6 and 0.7 cm^2/(V s) for PNDIT2-C20 and PNDIT2-C16, and $\mu_{sat,max}$ = 0.21 and 0.1 cm^2/(V s) for PNDFu2-C20 and PNDIFu2-C16, respectively.

As a result of the strong aggregation of PNDIFu2 in solution, directional alignment of films, driven by the orientation of fibrillar domains under flow-induced shear fields, can be readily achieved during the fast off-center spin-coating deposition, in analogy with the thiophene based analogous PNDIT2.[50] Figure 7 shows AFM height (a,c) and phase (b,d) images of PNDIT2-C20 (a,b) and PNDIFu2-C20 (c,d) films made from toluene followed by optimal thermal annealing processes (120 and 250 °C, respectively). Both films exhibit typical fibrillar-like morphologies with elongated domains mostly aligned along the flow direction as indicated by the red arrows. The small roughness of PNDIT2-C20 (R_{rms} = 0.4 nm) allows to distinguish fibrillary domains within the topography of the films (Figure 7a). A larger R_{rms} of 1.1 nm is measured on PNDIFu2-C20, mostly hiding fibrillar microstructure in the height image (Figure 7c), but clearly visible in the phase image (Figure 7d). Moreover, the superior aggregation of PNDIFu2 in solution, eventually induced by its more planar backbone, leads to stronger transport anisotropy of the resulting films. Whether this is caused by larger aggregates or a larger amount of aggregates poses an unsolved yet interesting question, which opens up possibilities for enhanced alignment of conjugated backbones in thin films. Regardless of this, our observations on PNDIFu2 films further confirm that alignment efficiency under shear fields depends on an intermediate step during the deposition, where preformed aggregates in solution form the seed for the film growth.[19,51]

Despite the enhanced alignment of PNDIFu2 chains in films, electron transport of PNDIFu2 is good but lower by a factor of ∼3 compared to the extensively studied PNDIT2. This may appear surprising since the combination of a more effective alignment and a more planarized backbone of PNDIFu2 are typically correlated with improved intrachain transport properties.[9,11] Moreover, the closer $\pi-\pi$ stacking distance observed in the ordered phase of PNDIFu2, which is also characterized by a higher coherence length in the (100) direction, should improve charge carrier mobility through enhanced interchain charge hopping if the interchain step was the bottleneck.

Apparently, these potentially beneficial parameters are counterbalanced by electronic effects induced by furan. In PNDIFu2, the polaron mainly relaxes over a single NDI unit, resulting in a higher electron reorganization energy with respect to PNDIT2, where polaron relaxation occurs at least over two

DOI: 10.1021/acs.chemmater.6b05313
Chem. Mater. 2017, 29, 5473−5483

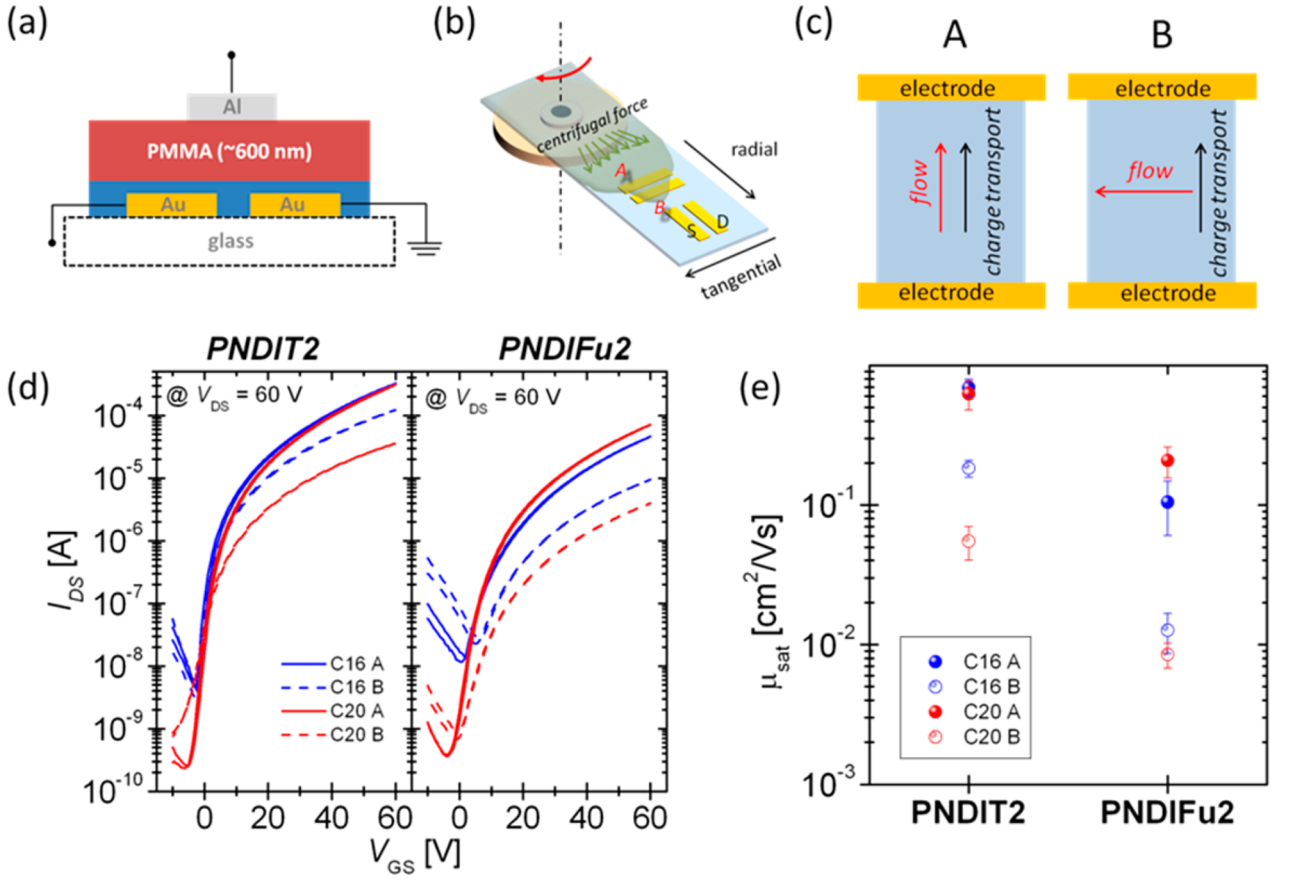

Figure 6. (a) Schematic of bottom contact top gate FETs; (b,c) sketch of off-center spin- coating deposition: A and B source and drain patterns allow to probe transport parallel (A) and perpendicular (B) to the direction of the flow and thus to the man chain direction; (d) transfer characteristics of individually optimized FETs: toluene for PNDIFu2-C20 and PNDIT2-C20, *o*-DCB for PNDIFu2-C16, and chlorobenzene for PNDIT2-C16; (e) plot of mean saturation mobility values (μ_{sat}). Before dielectric deposition, PNDIT2 and PNDIFu2 films underwent thermal annealing of 120 and 250 °C, respectively.

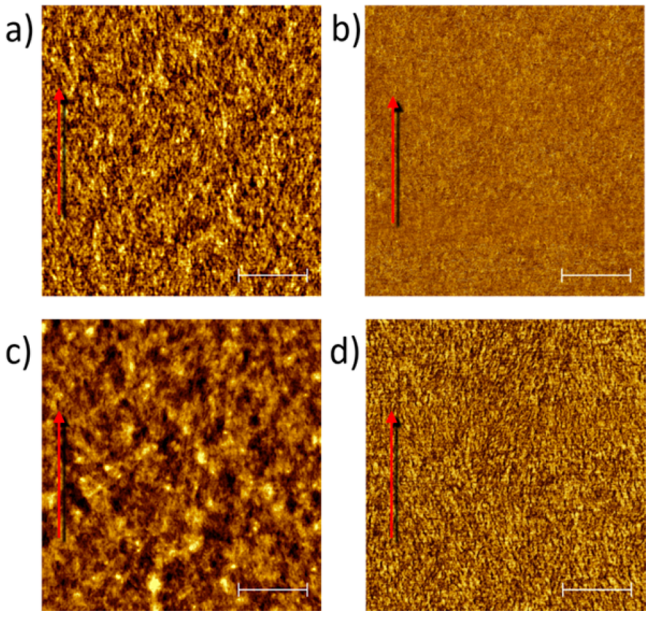

Figure 7. (a) AFM height (a,c) and phase (b,d) images of PNDIT2-C20 (a,b) and PNDIFu2-C20 (c,d) films spun from toluene and thermally annealed at the temperatures of charge transport optimization (120 °C for PNDIT2-C20 and 250 °C for PNDIFu2-C20). In all images, the scale bar is 500 nm.

repeat units. We speculate that the more electron-rich sulfur, having d-electrons, is at the origin of this behavior. The different polaron extension should lead to a higher energetic barrier for charge transfer in PNDIFu2 films, both at the interchain level, frustrating the effect of a closer $\pi-\pi$ stacking, and at the intrachain level, therefore limiting the benefit of structural alignment. While further studies are required to fully explain the transport differences between the two copolymers on more quantitative basis, our findings show that higher backbone planarity coupled with smaller $\pi-\pi$ stacking distances does not lead to improved transport properties *per se*. In this context, it appears interesting to investigate PNDISe2, which is the known analogous material with biselenophene as comonomer.[37]

3. CONCLUSION

Conjugated copolymers made of alternating naphthalene diimide and bifuran units PNDIFu2 can be synthesized using $NidpppCl_2$ catalyzed polymerization of radical anions. The effects of incorporating the bifuran unit into the copolymer backbone was thoroughly investigated for the two different side chains 2-hexyldecyl (C16) and 2-octyldodecyl (C20), and compared to the well-known analogue PNDIT2. PNDIFu2 showed a much more coplanar backbone due to reduced steric hindrance between the imide oxygen and the furan ring compared to thiophene. The oscillator strength of the low energy absorption band of PNDIFu2 is also enhanced

DOI: 10.1021/acs.chemmater.6b05313
Chem. Mater. 2017, 29, 5473−5483

compared to PNDIT2, making PNDIFu2 an interesting electron transporting material for usage also in all polymer solar cells with complementary absorbing donor polymers. The backbone planarization of PNDIFu2 can explain the observed stronger aggregation in solution with respect to PNDIT2, which eases directional alignment of polymer chains within aggregates using off-center spin-coating. As a consequence, optimized PNDIFu2 films show a markedly stronger transport anisotropy when tested in FETs, achieving a ratio of 18.3 for PNDIFu2-C20 for backbones aligned perpendicular and parallel to the electrodes. Overall, optimized FETs made from PNDIFu2 show a maximum electron field-effect mobility of 0.21 $cm^2/(V\ s)$, which is approximately three-times lower compared to the mobility of PNDIT2 under the same conditions. Thus, the greater backbone planarity, closer $\pi-\pi$ stacking distance, and stronger aggregation leading to enhanced anisotropy for PNDIFu2 do not result in superior charge transport properties compared to PNDIT2. A possible molecular-based reason for this unexpected behavior is a higher intramolecular reorganization energy of PNDIFu2 than in PNDIT2 owing to an enhanced polaron localization, which counterbalances the otherwise beneficial properties of PNDIFu2. This scenario offers clear directions for further improvement of charge transport in specifically designed and orientationally aligned donor−acceptor copolymers, in which, besides a planar ground state conformation, delocalization of charge excited states is required to benefit from uniaxial alignment thanks to improved intrachain transport.

■ ASSOCIATED CONTENT

Supporting Information

The Supporting Information is available free of charge on the ACS Publications website at DOI: 10.1021/acs.chemmater.6b05313.

Synthesis procedures, general information, additional UV−vis spectroscopy, polarized UV−vis spectroscopy, cyclic voltammetry, thermal analysis, additional GIWAXS data, additional electrical characterization, additional AFM images, and additional DFT calculations (PDF)

■ AUTHOR INFORMATION

Corresponding Authors

*E-mail: michael.sommer@chemie.uni-chemnitz.de.

*E-mail: mario.caironi@iit.it.

ORCID

Ullrich Steiner: 0000-0001-5936-339X

Mario Caironi: 0000-0002-0442-4439

Michael Sommer: 0000-0002-2377-5998

Present Address

○Technische Universität Chemnitz, Polymerchemie, Straße der Nationen 62, 09111 Chemnitz, Germany.

Notes

The authors declare no competing financial interest.

■ ACKNOWLEDGMENTS

M.S. and R.M. are grateful to the DFG (IRTG 1642 Soft Matter Science) for funding. Part of the work was conducted at beamline D1 at the Cornell High Energy Synchrotron Source (CHESS); CHESS is supported by the NSF & NIH/NIGMS via NSF award DMR-1332208. We thank D. Smilgies, X. Sheng, and J. Dolan for their help during the D1 experiment at CHESS. A. Hexemer is gratefully acknowledged for stimulating discussions. A. Hexemer and Xi-CAM are supported by the U.S. Department of Energy under Contract No. DE-AC02-05CH1123, the ECA award program, and the LBNL LDRD "TReXS". M.C. and A.L. acknowledge the financial support of the European Research Council (ERC) under the European Union's Horizon 2020 research and innovation programme "HEROIC", grant agreement 638059.

■ REFERENCES

(1) Facchetti, A. π-Conjugated Polymers for Organic Electronics and Photovoltaic Cell Applications. *Chem. Mater.* **2011**, *23* (3), 733−758.

(2) Rivnay, J.; Toney, M. F.; Zheng, Y.; Kauvar, I. V.; Chen, Z.; Wagner, V.; Facchetti, A.; Salleo, A. Unconventional Face-On Texture and Exceptional In-Plane Order of a High Mobility n-Type Polymer. *Adv. Mater.* **2010**, *22* (39), 4359−4363.

(3) Zhao, Y.; Guo, Y.; Liu, Y. 25th Anniversary Article: Recent Advances in n-Type and Ambipolar Organic Field-Effect Transistors. *Adv. Mater.* **2013**, *25* (38), 5372−5391.

(4) Nielsen, C. B.; Turbiez, M.; McCulloch, I. Recent Advances in the Development of Semiconducting DPP-Containing Polymers for Transistor Applications. *Adv. Mater.* **2013**, *25* (13), 1859−1880.

(5) Zhan, X.; Tan, Z.; Zhou, E.; Li, Y.; Misra, R.; Grant, A.; Domercq, B.; Zhang, X.-H.; An, Z.; Zhang, X.; Barlow, S.; Kippelen, B.; Marder, S. R. Copolymers of Perylene Diimide with Dithienothiophene and Dithienopyrrole as Electron-Transport Materials for All-Polymer Solar Cells and Field-Effect Transistors. *J. Mater. Chem.* **2009**, *19* (32), 5794−5803.

(6) Sommer, M. Conjugated Polymers Based on Naphthalene Diimide for Organic Electronics. *J. Mater. Chem. C* **2014**, *2* (17), 3088−3098.

(7) Kola, S.; Tremblay, N. J.; Yeh, M.-L.; Katz, H. E.; Kirschner, S. B.; Reich, D. H. Synthesis and Characterization of a Pyromellitic Diimide-Based Polymer with C- and N-Main Chain Links: Matrix for Solution-Processable n-Channel Field-Effect Transistors. *ACS Macro Lett.* **2012**, *1* (1), 136−140.

(8) Guo, X.; Watson, M. D. Pyromellitic Diimide-Based Donor−Acceptor Poly(Phenylene Ethynylene)S. *Macromolecules* **2011**, *44* (17), 6711−6716.

(9) Lei, T.; Xia, X.; Wang, J.-Y.; Liu, C.-J.; Pei, J. Conformation Locked" Strong Electron-Deficient Poly(p-Phenylene Vinylene) Derivatives for Ambient-Stable n-Type Field-Effect Transistors: Synthesis, Properties, and Effects of Fluorine Substitution Position. *J. Am. Chem. Soc.* **2014**, *136* (5), 2135−2141.

(10) Lei, T.; Dou, J.-H.; Cao, X.-Y.; Wang, J.-Y.; Pei, J. Electron-Deficient Poly(p-Phenylene Vinylene) Provides Electron Mobility over 1 Cm2 V−1 S−1 under Ambient Conditions. *J. Am. Chem. Soc.* **2013**, *135* (33), 12168−12171.

(11) Holliday, S.; Donaghey, J. E.; McCulloch, I. Advances in Charge Carrier Mobilities of Semiconducting Polymers Used in Organic Transistors. *Chem. Mater.* **2014**, *26* (1), 647−663.

(12) Ma, J.; Yin, L.; Zou, G.; Zhang, Q. Regioisomerically Pure 1,7-Dibromo-Substituted Perylene Bisimide Dyes: Efficient Synthesis, Separation, and Characterization. *Eur. J. Org. Chem.* **2015**, *2015* (15), 3296−3302.

(13) Guo, X.; Watson, M. D. Conjugated Polymers from Naphthalene Bisimide. *Org. Lett.* **2008**, *10* (23), 5333−5336.

(14) Matsidik, R.; Komber, H.; Luzio, A.; Caironi, M.; Sommer, M. Defect-Free Naphthalene Diimide Bithiophene Copolymers with Controlled Molar Mass and High Performance via Direct Arylation Polycondensation. *J. Am. Chem. Soc.* **2015**, *137* (20), 6705−6711.

(15) Yan, H.; Chen, Z.; Zheng, Y.; Newman, C.; Quinn, J. R.; Dötz, F.; Kastler, M.; Facchetti, A. A High-Mobility Electron-Transporting Polymer for Printed Transistors: Article: Nature. *Nature* **2009**, *457*, 679−686.

(16) Fazzi, D.; Caironi, M.; Castiglioni, C. Quantum-Chemical Insights into the Prediction of Charge Transport Parameters for a

DOI: 10.1021/acs.chemmater.6b05313
Chem. Mater. 2017, 29, 5473−5483

Naphthalenetetracarboxydiimide-Based Copolymer with Enhanced Electron Mobility. *J. Am. Chem. Soc.* **2011**, *133* (47), 19056−19059.
(17) Giussani, E.; Fazzi, D.; Brambilla, L.; Caironi, M.; Castiglioni, C. Molecular Level Investigation of the Film Structure of a High Electron Mobility Copolymer via Vibrational Spectroscopy. *Macromolecules* **2013**, *46* (7), 2658−2670.
(18) Martino, N.; Fazzi, D.; Sciascia, C.; Luzio, A.; Antognazza, M. R.; Caironi, M. Mapping Orientational Order of Charge-Probed Domains in a Semiconducting Polymer. *ACS Nano* **2014**, *8* (6), 5968−5978.
(19) Luzio, A.; Criante, L.; D'Innocenzo, V.; Caironi, M. Control of Charge Transport in a Semiconducting Copolymer by Solvent-Induced Long-Range Order. *Sci. Rep.* **2013**, *3*, 3425.
(20) Schuettfort, T.; Thomsen, L.; McNeill, C. R. Observation of a Distinct Surface Molecular Orientation in Films of a High Mobility Conjugated Polymer. *J. Am. Chem. Soc.* **2013**, *135* (3), 1092−1101.
(21) Wang, S.; Fabiano, S.; Himmelberger, S.; Puzinas, S.; Crispin, X.; Salleo, A.; Berggren, M. Experimental Evidence That Short-Range Intermolecular Aggregation Is Sufficient for Efficient Charge Transport in Conjugated Polymers. *Proc. Natl. Acad. Sci. U. S. A.* **2015**, *112* (34), 10599−10604.
(22) Szumilo, M. M.; Gann, E. H.; McNeill, C. R.; Lemaur, V.; Oliver, Y.; Thomsen, L.; Vaynzof, Y.; Sommer, M.; Sirringhaus, H. Structure Influence on Charge Transport in Naphthalenediimide−Thiophene Copolymers. *Chem. Mater.* **2014**, *26* (23), 6796−6804.
(23) Luzio, A.; Fazzi, D.; Nübling, F.; Matsidik, R.; Straub, A.; Komber, H.; Giussani, E.; Watkins, S. E.; Barbatti, M.; Thiel, W.; Gann, E.; Thomsen, L.; McNeill, C. R.; Caironi, M.; Sommer, M. Structure−Function Relationships of High-Electron Mobility Naphthalene Diimide Copolymers Prepared Via Direct Arylation. *Chem. Mater.* **2014**, *26* (21), 6233−6240.
(24) Guo, X.; Kim, F. S.; Seger, M. J.; Jenekhe, S. A.; Watson, M. D. Naphthalene Diimide-Based Polymer Semiconductors: Synthesis, Structure−Property Correlations, and n-Channel and Ambipolar Field-Effect Transistors. *Chem. Mater.* **2012**, *24* (8), 1434−1442.
(25) Kim, R.; Amegadze, P. S. K.; Kang, I.; Yun, H.-J.; Noh, Y.-Y.; Kwon, S.-K.; Kim, Y.-H. High-Mobility Air-Stable Naphthalene Diimide-Based Copolymer Containing Extended π-Conjugation for n-Channel Organic Field Effect Transistors. *Adv. Funct. Mater.* **2013**, *23* (46), 5719−5727.
(26) Kang, B.; Kim, R.; Lee, S. B.; Kwon, S.-K.; Kim, Y.-H.; Cho, K. Side-Chain-Induced Rigid Backbone Organization of Polymer Semiconductors through Semifluoroalkyl Side Chains. *J. Am. Chem. Soc.* **2016**, *138* (11), 3679−3686.
(27) Naceur, B. M.; Gandini, A. *Monomers, Polymers and Composites from Renewable Resources*; Elsevier: Oxford, U.K., 2008.
(28) Gandini, A. Polymers from Renewable Resources: A Challenge for the Future of Macromolecular Materials. *Macromolecules* **2008**, *41* (24), 9491−9504.
(29) Gidron, O.; Bendikov, M. α-Oligofurans: An Emerging Class of Conjugated Oligomers for Organic Electronics. *Angew. Chem., Int. Ed.* **2014**, *53* (10), 2546−2555.
(30) Yiu, A. T.; Beaujuge, P. M.; Lee, O. P.; Woo, C. H.; Toney, M. F.; Fréchet, J. M. J. Side-Chain Tunability of Furan-Containing Low-Band-Gap Polymers Provides Control of Structural Order in Efficient Solar Cells. *J. Am. Chem. Soc.* **2012**, *134* (4), 2180−2185.
(31) Matsidik, R.; Martin, J.; Schmidt, S.; Obermayer, J.; Lombeck, F.; Nübling, F.; Komber, H.; Fazzi, D.; Sommer, M. C−H Arylation of Unsubstituted Furan and Thiophene with Acceptor Bromides: Access to Donor−Acceptor−Donor-Type Building Blocks for Organic Electronics. *J. Org. Chem.* **2015**, *80* (2), 980−987.
(32) Huang, P.; Du, J.; Biewer, M. C.; Stefan, M. C. Developments of Furan and Benzodifuran Semiconductors for Organic Photovoltaics. *J. Mater. Chem. A* **2015**, *3* (12), 6244−6257.
(33) Xiong, Y.; Tao, J.; Wang, R.; Qiao, X.; Yang, X.; Wang, D.; Wu, H.; Li, H. A Furan−Thiophene-Based Quinoidal Compound: A New Class of Solution-Processable High-Performance n-Type Organic Semiconductor. *Adv. Mater.* **2016**, *28*, 5949−5953.
(34) Liu, J.; Walker, B.; Tamayo, A.; Zhang, Y.; Nguyen, T.-Q. Effects of Heteroatom Substitutions on the Crystal Structure, Film Formation, and Optoelectronic Properties of Diketopyrrolopyrrole-Based Materials. *Adv. Funct. Mater.* **2013**, *23* (1), 47−56.
(35) Hendsbee, A. D.; Sun, J.-P.; McCormick, T. M.; Hill, I. G.; Welch, G. C. Unusual Loss of Electron Mobility upon Furan for Thiophene Substitution in a Molecular Semiconductor. *Org. Electron.* **2015**, *18*, 118−125.
(36) Bijleveld, J. C.; Karsten, B. P.; Mathijssen, S. G. J.; Wienk, M. M.; de Leeuw, D. M.; Janssen, R. A. J. Small Band Gap Copolymers Based on Furan and Diketopyrrolopyrrole for Field-Effect Transistors and Photovoltaic Cells. *J. Mater. Chem.* **2011**, *21* (5), 1600−1606.
(37) Hwang, Y.-J.; Murari, N. M.; Jenekhe, S. A. New N-Type Polymer Semiconductors Based on Naphthalene Diimide and Selenophene Derivatives for Organic Field-Effect Transistors. *Polym. Chem.* **2013**, *4*, 3187−3195.
(38) Senkovskyy, V.; Tkachov, R.; Komber, H.; Sommer, M.; Heuken, M.; Voit, B.; Huck, W. T. S.; Kataev, V.; Petr, A.; Kiriy, A. Chain-Growth Polymerization of Unusual Anion-Radical Monomers Based on Naphthalene Diimide: A New Route to Well-Defined n-Type Conjugated Copolymers. *J. Am. Chem. Soc.* **2011**, *133* (49), 19966−19970.
(39) Qiu, Y.; Fortney, A.; Tsai, C.-H.; Baker, M. A.; Gil, R. R.; Kowalewski, T.; Noonan, K. J. T. Synthesis of Polyfuran and Thiophene-Furan Alternating Copolymers Using Catalyst-Transfer Polycondensation. *ACS Macro Lett.* **2016**, *5* (3), 332−336.
(40) Tkachov, R.; Karpov, Y.; Senkovskyy, V.; Raguzin, I.; Zessin, J.; Lederer, A.; Stamm, M.; Voit, B.; Beryozkina, T.; Bakulev, V.; Zhao, W.; Facchetti, A.; Kiriy, A. Efficient Tin-Free Route to a Donor−Acceptor Semiconducting Copolymer with Variable Molecular Weights. *Macromolecules* **2014**, *47* (12), 3845−3851.
(41) Caddeo, C.; Fazzi, D.; Caironi, M.; Mattoni, A. Atomistic Simulations of P(NDI2OD-T2) Morphologies: From Single Chain to Condensed Phases. *J. Phys. Chem. B* **2014**, *118* (43), 12556−12565.
(42) Steyrleuthner, R.; Schubert, M.; Howard, I.; Klaumünzer, B.; Schilling, K.; Chen, Z.; Saalfrank, P.; Laquai, F.; Facchetti, A.; Neher, D. Aggregation in a High-Mobility n-Type Low-Bandgap Copolymer with Implications on Semicrystalline Morphology. *J. Am. Chem. Soc.* **2012**, *134* (44), 18303−18317.
(43) Fazzi, D.; Caironi, M. Multi-Length-Scale Relationships between the Polymer Molecular Structure and Charge Transport: The Case of Poly-Naphthalene Diimide Bithiophene. *Phys. Chem. Chem. Phys.* **2015**, *17* (14), 8573−8590.
(44) Troisi, A. Charge Transport in High Mobility Molecular Semiconductors: Classical Models and New Theories. *Chem. Soc. Rev.* **2011**, *40* (5), 2347−2358.
(45) Stafström, S. Electron Localization and the Transition from Adiabatic to Nonadiabatic Charge Transport in Organic Conductors. *Chem. Soc. Rev.* **2010**, *39* (7), 2484−2499.
(46) Fratini, S.; Mayou, D.; Ciuchi, S. The Transient Localization Scenario for Charge Transport in Crystalline Organic Materials. *Adv. Funct. Mater.* **2016**, *26* (14), 2292−2315.
(47) Rühle, V.; Kirkpatrick, J.; Andrienko, D. A Multiscale Description of Charge Transport in Conjugated Oligomers. *J. Chem. Phys.* **2010**, *132* (13), 134103.
(48) Kubař, T.; Elstner, M.; Popescu, B.; Kleinekathöfer, U. Polaron Effects on Charge Transport through Molecular Wires: A Multiscale Approach. *J. Chem. Theory Comput.* **2017**, *13* (1), 286−296.
(49) Rivnay, J.; Steyrleuthner, R.; Jimison, L. H.; Casadei, A.; Chen, Z.; Toney, M. F.; Facchetti, A.; Neher, D.; Salleo, A. Drastic Control of Texture in a High Performance N-Type Polymeric Semiconductor and Implications for Charge Transport. *Macromolecules* **2011**, *44* (13), 5246−5255.
(50) Bucella, S. G.; Luzio, A.; Gann, E.; Thomsen, L.; McNeill, C. R.; Pace, G.; Perinot, A.; Chen, Z.; Facchetti, A.; Caironi, M. Macroscopic and High-Throughput Printing of Aligned Nanostructured Polymer Semiconductors for MHz Large-Area Electronics. *Nat. Commun.* **2015**, *6*, 8394.

DOI: 10.1021/acs.chemmater.6b05313
Chem. Mater. 2017, 29, 5473−5483

(51) Kim, N.-K.; Jang, S.-Y.; Pace, G.; Caironi, M.; Park, W.-T.; Khim, D.; Kim, J.; Kim, D.-Y.; Noh, Y.-Y. High-Performance Organic Field-Effect Transistors with Directionally Aligned Conjugated Polymer Film Deposited from Pre-Aggregated Solution. *Chem. Mater.* **2015**, *27* (24), 8345−8353.
(52) Schuettfort, T.; Huettner, S.; Lilliu, S.; Macdonald, J. E.; Thomsen, L.; McNeill, C. R. Surface and Bulk Structural Characterization of a High-Mobility Electron-Transporting Polymer. *Macromolecules* **2011**, *44* (6), 1530−1539.
(53) Tremel, K.; Fischer, F. S. U.; Kayunkid, N.; Pietro, R. D.; Tkachov, R.; Kiriy, A.; Neher, D.; Ludwigs, S.; Brinkmann, M. Charge Transport Anisotropy in Highly Oriented Thin Films of the Acceptor Polymer P(NDI2OD-T2). *Adv. Energy Mater.* **2014**, *4* (10), 1301659.
(54) Kim, B.-G.; Jeong, E. J.; Chung, J. W.; Seo, S.; Koo, B.; Kim, J. A Molecular Design Principle of Lyotropic Liquid-Crystalline Conjugated Polymers with Directed Alignment Capability for Plastic Electronics. *Nat. Mater.* **2013**, *12* (7), 659−664.

DOI: 10.1021/acs.chemmater.6b05313
Chem. Mater. 2017, 29, 5473−5483